Doping and intermixing in CdS/CdTe solar cells fabricated under different conditions

U. Jahn[a)]
Paul-Drude-Institut für Festkörperelektronik, Hausvogteiplatz 5-7, 10117 Berlin, Germany

T. Okamoto, A. Yamada, and M. Konagai
Department of Physical Electronics, Tokyo Institute of Technology, 2-12-1 O-okayama, Meguro-ku, Tokyo 152-8552, Japan

(Received 31 January 2001; accepted for publication 29 May 2001)

Thin film CdS/CdTe solar cell structures have been investigated by spatially resolved cathodoluminescence (CL) spectroscopy. A postgrowth $CdCl_2$ treatment of the CdTe layer was found to homogenize the distribution of acceptor-like defects or impurities leading to optimized *p*-type conversion of the polycrystalline CdTe. For values of the growth temperature (T_G) of about 600 °C, the intermixed region between the CdS layer and CdTe grains is surprisingly thin. However, for T_G as large as 630–650 °C, a gradual decrease of the CdTe band gap due to sulfur intermixing appears to be present up to 0.6 μm from the CdS/CdTe interface. The CL spectra of the CdS window layer exhibit two broad bands centered at 1.72 (red) and 2.04 eV (yellow). The yellow one is quenched by the $CdCl_2$ treatment, indicating passivation or promoted outdiffusion of Cd interstitials.
© *2001 American Institute of Physics.* [DOI: 10.1063/1.1388565]

I. INTRODUCTION

One of the promising material systems for solar cell mass production is the glass/transparent and conductive oxide (TCO)/*n*-CdS/*p*-CdTe structure. Substantial advancement with regard to the enhancement of the conversion efficiency was linked to the application of a postdeposition $CdCl_2$ treatment of the CdTe layers that led to conversion efficiencies as high as 15.8% at the beginning of the 1990s.[1] Since that time, no remarkable improvements towards the predicted possible efficiency of about 29% (Ref. 2) could be achieved. Thus, a more detailed physical understanding of the correlation between material treatment and device performance seems to be essential for further progress. Four key areas are stressed in which advances are urgently needed.[3] They are related to the CdTe doping in connection with $CdCl_2$ processing, to interface and grain boundary effects, to the development of stable contacts with low barriers, and to the question of how different processing steps influence each other. To address problems like these, probes of electronic properties with submicrometer resolution are desirable because of the polycrystalline nature of these layers.

Spatially resolved optical and electron beam induced current (OBIC and EBIC) investigations have been performed in detail by Edwards *et al.*[4] The $CdCl_2$ treatment was found to cause homogenization of the EBIC response and passivation of grain boundaries. Moreover, a change of the grain boundary contrast of EBIC images with increasing excitation density indicates an enhancement of apparent *p* doping near the grain boundaries. EBIC images are, however, difficult to interpret, particularly for a system as complex as the polycrystalline CdS/CdTe solar cell, where in addition to lateral variation of the distribution of carrier traps, doping concentrations, and the depletion layer width the occurrence of both lateral and vertical $p-n$ junctions can be expected.[5] In this work, the cathodoluminescence (CL) mode of a scanning electron microscope (SEM) is employed. We used in particular the spectral peak position of distinct bound excitons to obtain direct information about the lateral doping distribution and changes of the CdTe band width due to sulfur intermixing near the CdS/CdTe interface. Local excitation with spatial resolution of about 300 nm allows inspection of single CdTe grains as well as of the CdS/CdTe interface region. Moreover, satisfactory CL spectra could be obtained even for the thin CdS window layer at cleaved edges of solar cell structures and they were suitable for investigating the electronic properties of this layer for different treatment conditions. A correlation among fabrication conditions, the distribution (spectral and spatial) of exciton lines, and device performance could be found.

II. EXPERIMENTAL PROCEDURE

Two types of samples have been investigated. In order to correlate various fabrication conditions with achieved device parameters, the first type consists of complete CdTe thin film solar cells. They are composed of 6–8 μm *p*-type CdTe layers deposited by close spaced sublimation (CSS) on a glass (Corning 1737) substrate with a 250-nm-thick indium–tin–oxide (ITO) film and a 60–80 nm CdS window layer. More details about the fabrication procedure can be found elsewhere.[6,7] CL spectra were obtained at cleaved edges of those devices. In order to enable CL excitation of the free CdTe surface and to improve the cleavage of respective layer structures, the second type of samples consists of CdS (90 nm)/CdTe (6 μm) layers deposited on Si substrates under conditions comparable to those of the complete devices. CL spectra and images were recorded at cleaved edges and from

a)Electronic mail: ujahn@pdi-berlin.de

 © 2001 American Institute of Physics

Downloaded 18 Jun 2004 to 62.141.165.57. Redistribution subject to AIP license or copyright, see http://jap.aip.org/jap/copyright.jsp

TABLE I. Substrate temperature during the CdTe deposition (T_G), temperature of the $CdCl_2$ treatment (T_{CdCl_2}), and conversion efficiency of the samples investigated.

Si/CdS/CdTe structures			Glass/ITO/CdS/CdTe/C/Ag structures			
Sample No.	T_G (°C)	T_{CdCl_2} (°C)	Sample No.	T_G (°C)	T_{CdCl_2} (°C)	Efficiency (%)
1	600	Without	4	595	Without	5.8
2	600	460	5	595	460	7.1
3	600	415	6	610	415	13.7
			7	630	415	14.1
			8	650	415	12.7

the CdTe surface of those samples. For both the cleaved edge and surface inspection, we performed CL measurements on unpolished samples to prevent the influence of polish-related defects or changes in strain of the electronic properties of the material. In Table I, the most essential fabrication conditions are summarized along with the resulting conversion efficiencies of the respective solar cells. The substrate temperature (T_G) during the CdTe deposition and the $CdCl_2$ treatment conditions have been varied. For nearly constant values of T_G, the conversion efficiency is very strongly influenced by the $CdCl_2$ treatment conditions. We found an optimum conversion efficiency for a treatment temperature of 415 °C. When the $CdCl_2$ treatment is kept at the optimum condition, the efficiency starts to decrease for values of T_G exceeding 630 °C. Consequently, the investigations to be discussed below are related to effects of both the $CdCl_2$ treatment and of the deposition temperature on the spatial and spectral cathodoluminescence distribution in selected samples.

CL spectra, line profiles, and images were obtained in a SEM equipped with an Oxford mono-CL2 and He-cooling stage system. A grating monochromator and a cooled photomultiplier as well as a charge coupled device (CCD) photodetector, respectively, were used to disperse and detect the CL signal. The electron beam energy was chosen to be 5 keV, and the current was to 0.1–1 nA. The sample temperature was usually set to 5 K.

III. EXPERIMENTAL RESULTS AND DISCUSSION

A. Doping and $CdCl_2$ treatment

CL spectra near the surface region of as-grown CdTe on a Si/CdS substrate are shown in Fig. 1. For the solid line, the excitation was averaged over an area of $20\times20\,\mu m^2$. This CL spectrum is rather broad and different excitonic contributions can hardly be distinguished. However, if the excitation is restricted by the focused electron beam to single CdTe grains like for the CL spectra depicted by symbols, distinct excitonic lines are well resolved. The arrows point to spectral positions of different excitonic transitions of CdTe, in which at 1.5965 eV the free exciton with $n=1$, at 1.586–1.588 and 1.590 eV acceptor bound excitons, and at 1.592–1.594 eV the donor bound excitons are expected to appear.[8–10] Consequently, each of the excited grains contains different types of impurities or defects acting as donors or acceptors. In as-grown CdTe layers, the spectral position of the exciton lines seems to be randomly distributed among various grains and even within a single grain.

$CdCl_2$ treatment results in rearrangement of the exciton distribution, indicating a doping effect. Figure 2 depicts SEM micrograph and CL spectra recorded for a number of spot excitations along a certain path connecting two neighboring grains (cf. the dotted arrow in the SEM image). The left-to-right scan of the excitation corresponds to the bottom-to-top ordering of the CL spectra. As can be clearly seen for the small grain (left-hand side) in Fig. 2, all the CL spectra are dominated by acceptor bound excitons (X_{A1},X_{A2}), whereas in the large grain (right-hand side) all the CL spectra are dominated by the donor bound exciton (X_D). The CL spectra in Fig. 2 reflect a general trend observed for many grains in $CdCl_2$-treated samples: small grains and the periphery of large grains are dominated by *p*-type doping, whereas the center of large grains is dominated by *n*-type doping.

The effect of the $CdCl_2$ treatment on the general doping distribution becomes more clearly visible in Fig. 3 which shows secondary electron (SE) and CL images of an as-grown and of a $CdCl_2$-treated CdTe layer. The SE images in Figs. 3(a) and 3(d) prove that most of the grains are twinned,

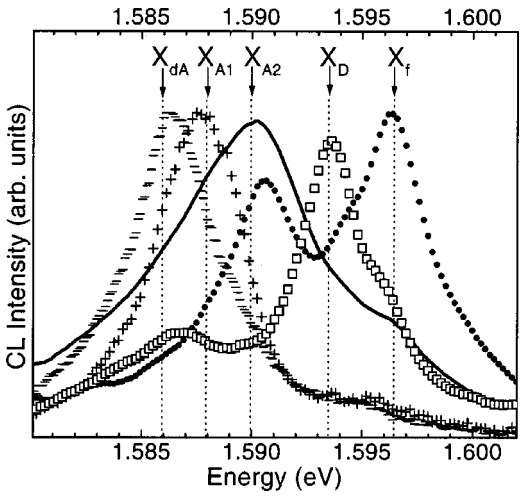

FIG. 1. CL spectra of a polycrystalline CdTe layer for an excitation area of $20\times20\,\mu m^2$ (solid line) and for spot excitation with the focused electron beam centered on several distinct CdTe grains (symbols). X_f, X_D, X_{A1}, X_{A2}, and X_{dA} mark the peak positions of the free, donor bound, acceptor bound (acceptors *A*1, *A*2, and deep acceptor) excitons, respectively.

Downloaded 18 Jun 2004 to 62.141.165.57. Redistribution subject to AIP license or copyright, see http://jap.aip.org/jap/copyright.jsp

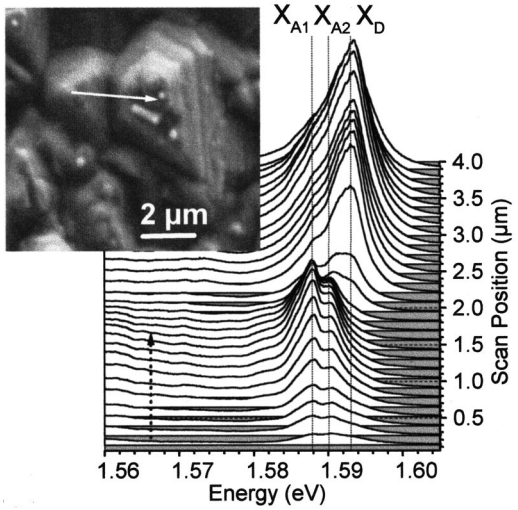

FIG. 2. SEM image and CL spectra of a $CdCl_2$-treated CdS/CdTe structure on Si. The CL spectra were excited at various spots along a path corresponding to the dotted arrow indicated in the SEM image. The left-hand side of the path is equal to the scan position zero.

indicating a high density of extended defects. In Figs. 3(b) and 3(e), the CL detection energy was set to the peak position of the donor bound exciton and in Figs. 3(c) and 3(f) to 1.585 eV (low energy side of the acceptor bound excitons). While for both samples without and with $CdCl_2$ treatment the donor bound exciton is essentially restricted to the center of large grains, CL from acceptor bound excitons is detected for almost every grain of the excited area and from the periphery of large grains only after $CdCl_2$ treatment.[11] This result shows directly the conversion of polycrystalline CdTe to a continuous *p*-type layer as a result of the $CdCl_2$ treatment, which has been generally established by various authors (see,

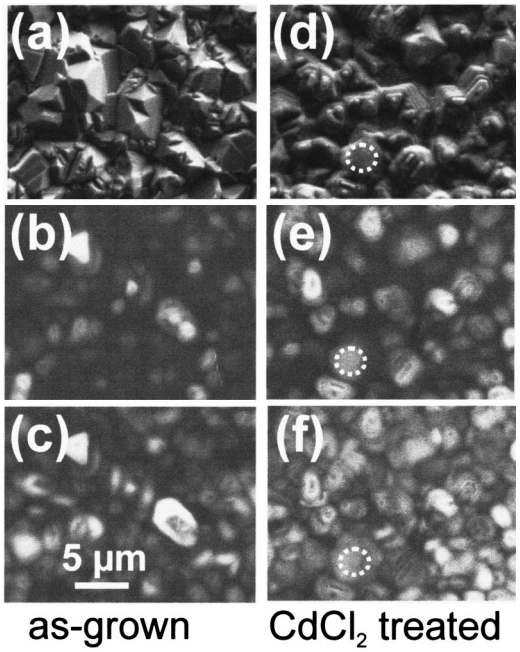

FIG. 3. Secondary electron (a), (d) and CL (b), (c), (e), (f) images of CdTe layers. For (b) and (e) the CL detection energy was set to 1.592 eV, while for (c) and (f) it was set to 1.585 eV.

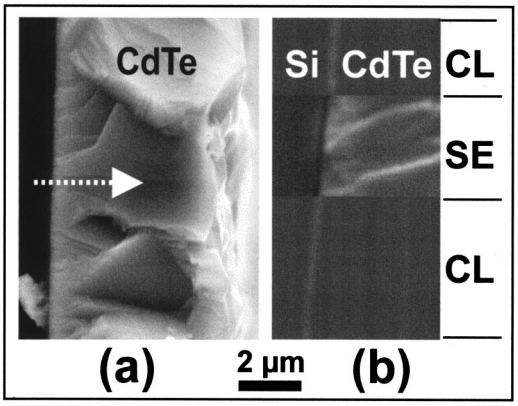

FIG. 4. SE image (a) and combined SE/CL image (b) of the cleaved edge of an as-grown CdS/CdTe structure deposited on Si. In (a), the dotted arrow marks the path along which the spectra of Fig. 5 have been excited. For the CL signal in (b), the detection energy was set to 1.7 eV.

e.g., the work of Durose *et al.*).[3] It suggests that chlorine is involved in the mechanism of the *p*-type conversion. At an early stage of technology development of CdS/CdTe solar cells, a postdeposition heat treatment of the CdTe layer was proven to initiate a *p*-type conversion by the generation of Cd vacancies, which act as native acceptors in CdTe.[12,13] From a theoretical point of view, the presence of chlorine is predicted to further promote *p*-type doping of CdTe by the formation of a Cd vacancy–chlorine complex, whose ionization energy is expected to be even 30 meV below that of the Cd vacancy.[14] Therefore, we assume that chlorine diffusion into small grains and within a border region of large grains during the $CdCl_2$ treatment promotes *p*-type conversion of the CdTe layers, which is correlated with a remarkable increase of the conversion efficiency of the solar cells by more than a factor of 2 (cf. Table I).

B. Intermixing at the CdS/CdTe interface region

In the following, the spectral peak position of the excitonic luminescence is used to probe the interface region between the CdS window layer and the CdTe absorber layer. Respective CL investigations were performed at the cleaved edge of CdTe layers deposited on Si/CdS substrates and of complete solar cell devices on glass/ITO/CdS substrates (see Table I). Figure 4(a) depicts a SE image of a cleaved Si/CdS/CdTe layer structure. In order to probe the properties of the *n*-CdS/*p*-CdTe interface, CL spectra are acquired along a line perpendicular to the layers crossing the Si/CdS/CdTe region (cf. the dotted arrow). For investigations like this, smoothly cleaved, large grains have been chosen so that the following consideration refers to features of CdTe grains and their interface with respect to the CdS layer. Because of the large size of the grains the CL line profiles are not affected by grain boundary effects. Figure 5 shows a set of CL spectra of an as-grown Si/CdS/CdTe system. The scan starts at the substrate (scan position zero) and ends in the CdTe layer. As it approaches the CdS/CdTe interface, the electron beam excitation first generates a broad CL spectrum in an energy range far above the CdTe band gap (for $E > 1.6$ eV). This CL signal appears independent of the respective substrate (Si/

Downloaded 18 Jun 2004 to 62.141.165.57. Redistribution subject to AIP license or copyright, see http://jap.aip.org/jap/copyright.jsp

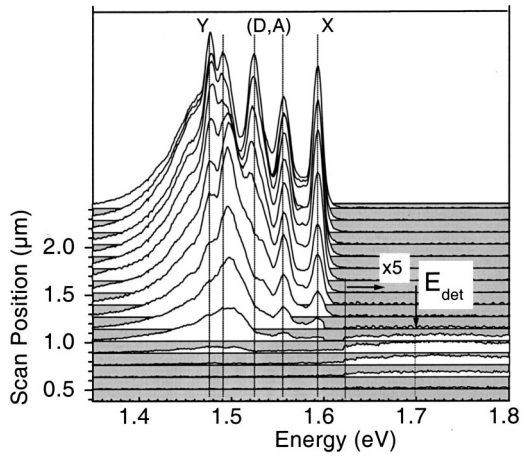

FIG. 5. CL spectra of the cleaved edge of an as-grown CdS/CdTe structure deposited on Si. The spectra were excited at various spots along the path marked by a dotted arrow in Fig. 4(a).

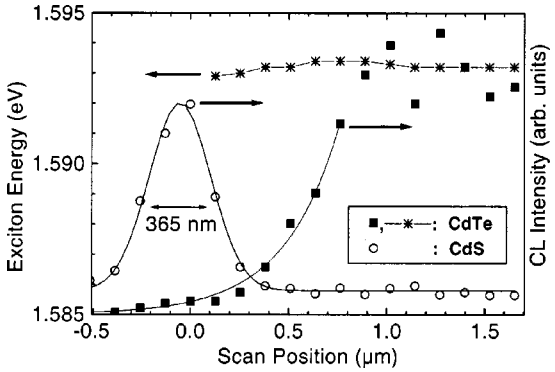

FIG. 6. Integrated intensities of the CdTe exciton (squares) and CdS-related CL (circles) as well as the spectral position of the CdTe exciton line (stars) as a function of the scan position. The data were extracted from Fig. 5.

CdS or glass/ITO/CdS) if the electron beam passes the region very close to the interface. Figure 4(b) shows a combined CL/SE image of the cleaved edge of a Si/CdS/CdTe structure. While the electron beam was scanning downwards, the signal was switched between the CL (detection energy: 1.7 eV) and SE signal. A comparison of the three parts of the image clearly confirms that the CL signal at 1.7 eV arises exclusively from the interface region between the substrate and CdTe layer, thus suggesting that this part of the spectrum originates from the thin CdS window layer. Its nature is briefly discussed below. For the moment, we only stress the importance of the CdS related CL as a marker of the CdS/CdTe interface position with regard to the scan position of the electron beam.

Immediately after passing the CdS layer, the usually observed luminescence lines of the near band gap range of CdTe—bound exciton at about 1.59 eV and (*D*, *A*) pair at about 1.55 eV—appear without any noticeable spectral shift. The exciton CL lines are strongly quenched near the interface, which is probably caused by interface states and/or by the electrical field within the depletion layer of the $p-n$ junction. Far from the interface, additional distinct CL lines appear, which are connected with different (*D*, *A*) pairs and the so-called *Y* luminescence at 1.477 eV. The latter is due to dislocations in the CdTe crystal.[15] Decreasing the distance with respect to the interface causes a rapid decrease of the CL intensities at 1.52 and 1.475 eV, leaving a broad CL band centered at about 1.5 eV for the interface region. These ''near-interface spectra'' closely resemble the photoluminescence (PL) spectra obtained by junction excitation.[6]

Figure 6 summarizes the data of Fig. 5 and provides an experimental estimate of the lateral resolution of the electron beam probe under the applied conditions ($T=5$ K, electron beam energy$=5$ keV). The circles and closed squares denote the integrated intensities of the CdS-related and CdTe-exciton CL, respectively. The stars indicate the spectral position of the exciton line as a function of the scan position with regard to the CdS layer (scan position zero). Since the thickness of the CdS layer (90 nm) is smaller than the expected diameter of the excitation volume, the profile of this layer cannot be resolved. We obtain a Gaussian shaped profile with a full width at half maximum (FWHM) of 365 nm, indicating lateral resolution of the CL mode of about 300 nm. This value is in accordance with an estimated diameter of the electron scattering volume of about 200 nm and a minority carrier diffusion length, which is expected to be considerably smaller than 300 nm at 5 K.[4] With the current spatial resolution, a decrease of the exciton peak position, i.e., a reduction of the CdTe bandwidth due to intermixing at the CdS/CdTe interface, cannot be observed in the as-grown sample.

In Fig. 7(a), scans such as the one in Fig. 6 are compared for samples experiencing different growth and $CdCl_2$ treatment conditions. As can be clearly seen, a $CdCl_2$ treatment—even for temperatures up to 460 °C—does not significantly

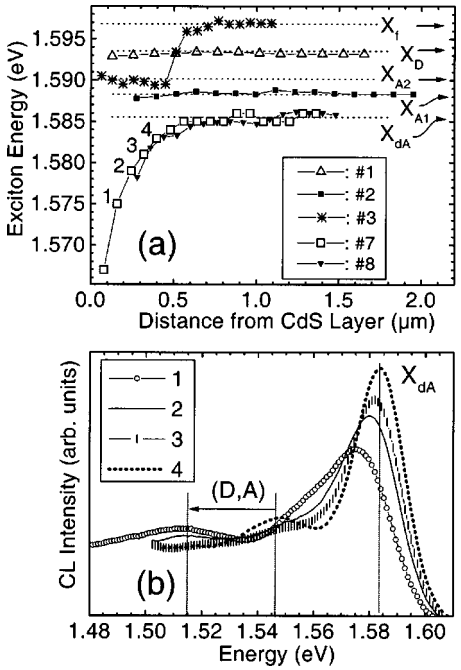

FIG. 7. (a) Spectral peak position of the CdTe exciton line as a function of the distance from the CdS layer for different $CdCl_2$ treatment conditions and substrate temperatures during the CdTe deposition. The treatment parameters for sample Nos. 1–8 are listed in Table I. X_f, X_D, X_{A1}, X_{A2}, and X_{dA} mark the peak positions of the free, donor bound, acceptor bound (acceptors *A*1, *A*2, and deep acceptor) excitons, respectively. (b) CL spectra at the scan positions are marked 1–4 in (a).

Downloaded 18 Jun 2004 to 62.141.165.57. Redistribution subject to AIP license or copyright, see http://jap.aip.org/jap/copyright.jsp

promote intermixing at the interface. The jump of the exciton energy of the sample treated at 415 °C (stars) from 1.5965 down to 1.590 eV near the interface is, rather, due to an inhomogeneous doping distribution within the respective grain (coexistence of regions dominated by free excitons with those dominated by acceptor bound ones) than to an abrupt narrowing of the band gap. As discussed above, the $CdCl_2$ treatment essentially affects the doping of the CdTe, which is reflected by an overall decrease of the peak energy of the excitonic CL within the probed grains after $CdCl_2$ treatment, particularly for higher values of T_{CdCl_2}.

An increase of the growth temperature, however, leads to a noticeable gradual redshift of the exciton energy down to values for which bound exciton levels are not expected in CdTe. This increasing redshift with decreasing distance to the interface is obviously due to an intermixed layer, whose thickness increases considerably if T_G becomes larger than 600 °C. Furthermore, at the highest deposition temperature, an overall lowering of the exciton energy down to 1.585 eV was observed. This excitonic energy level has been assigned to a deep-acceptor bound exciton associated with Cd vacancies.[8] Consequently, a CdTe deposition at substrate temperatures higher than 600 °C promotes both the formation of a rather thick intermixed layer and the generation of Cd vacancies. Note again that the results discussed refer to the CdTe grains rather than to grain boundary effects.

With regard to the content of sulfur within the intermixed layer, we have to take into account the fact that the CL signal is averaged over a layer thickness of about 300 nm. Consequently, the amount of sulfur cannot be determined directly from the exciton peak position. Nevertheless, considering the shape of the spectra—instead of only the peak position—the composition range of the interface region can roughly be estimated. Figure 7(b) shows four CL spectra of the CdTe layer grown at 630 °C for various distances of the exciting electron beam with respect to the CdS layer. Spectra 1–4 correspond to the exciton peak positions marked 1–4 in Fig. 7(a). As it approaches the CdS/CdTe interface, the redshift of the exciton peak position is accompanied by broadening of the spectrum, which is more pronounced on the low-energy side. The low-energy tail of the spectrum represents regions with a large CdS mole fraction. The exciton spectrum at position 1 extends down to about 1.55 eV. Taking into consideration a value of the exciton energy in the unmixed CdTe of 1.585 eV (the saturation level for large distances), we estimate a narrowing of the band gap of about 35 meV. This value is consistent with the observed shift of the (*D*, *A*) pair band from 1.55 (unmixed CdTe) down to 1.515 eV. A reduction of the CdTe band gap energy of 35 meV corresponds to a CdS mole fraction of 0.037.[16] Similar results were obtained by Grecu and Compaan[17] using junction PL of CdS/CdTe solar cells on commercial glass/SnO_2 substrates.

Since alloy formation could not be proven for $T_G = 600$ °C, while for higher values of T_G it was observed only for distances from the interface comparable to the lateral resolution, the intermixed layers inside the CdTe grains are probably very thin. If we take into account the maximum values of the diffusivity of sulfur in single crystal CdTe found by Lane *et al.*,[18] we obtain diffusion lengths of about 20 and 60 nm for sulfur in CdTe at 600 (30 s) and 650 °C (60 s), respectively [the T_G (time) values correspond to our deposition conditions]. From this result, we conclude that spatially integrated experiments revealing intermixed layers as thick as several 100 nm or a few μm are most probably influenced by faster diffusion of sulfur in the grain boundaries and extended defects.[3,19]

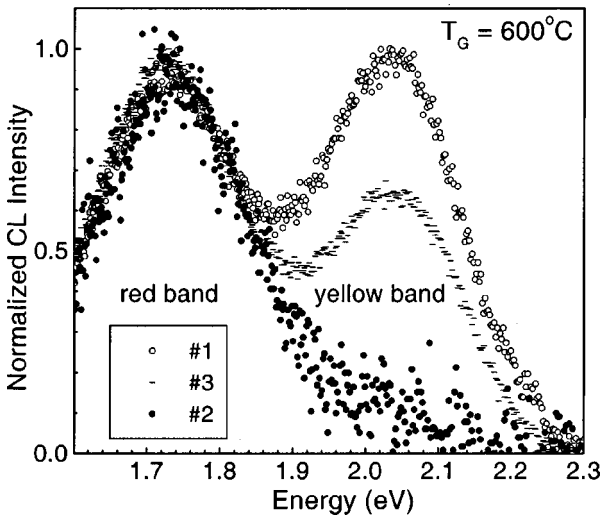

FIG. 8. CL spectra of the CdS window layer excited at the cleaved edge of a CdS (90 nm)/CdTe (6 μm) structure for different $CdCl_2$ treatment conditions (sample No. 1: untreated; Sample Nos. 2 and 3: treated at 460 and 415 °C, respectively).

C. CdS window layer

For excitation within the interface region, we obtained a CL signal at photon energies far above the CdTe band gap, which can be assigned to the thin CdS window layer (cf. Fig. 5). The whole spectral range of this CL is depicted in Fig. 8. Three spectra are shown that differ in $CdCl_2$ treatment conditions. They consist of two broad bands centered at 1.72 (red) and 2.04 eV (yellow). The intensities are normalized to the respective peak intensity of the red band. Agata *et al.*,[20] who investigated luminescence properties of gas-evaporated CdS, also found a red and a yellow PL band in microcrystals of 72 nm average size. These authors assigned the red band to transitions of electrons trapped at surface states to the valence band and the yellow one to a deep donor to valence band transition with Cd interstitials as the donors. Kulp[21] performed electron bombardment experiments on single crystal CdS and identified the luminescence bands at 1.72 and 2.04 eV as due to the sulfur vacancy and Cd interstitial, respectively. Thus, the yellow band can be undoubtedly assigned to the Cd interstitial. The intensity of this CL band is strongly reduced and it almost completely disappears after $CdCl_2$ treatment at 415 and 460 °C, respectively. Since after $CdCl_2$ treatment a considerable chlorine accumulation at the interface has been observed by several authors,[19,22] some effect of such a treatment on the CdS layer can be expected. Therefore, it is suggested that Cd interstitials are passivated or their outdiffusion is promoted by $CdCl_2$ treatment. In Fig. 9, the ratios of the integrated CL intensities of the red and

Downloaded 18 Jun 2004 to 62.141.165.57. Redistribution subject to AIP license or copyright, see http://jap.aip.org/jap/copyright.jsp

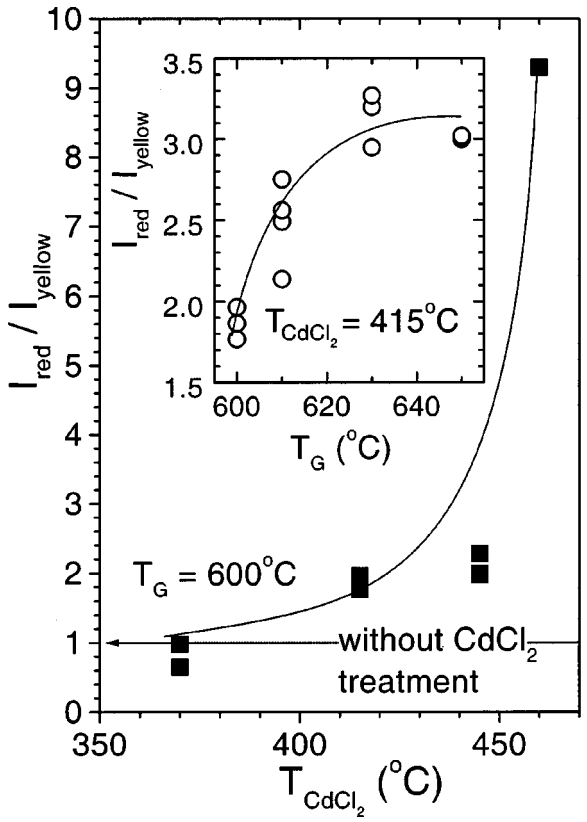

FIG. 9. Ratio between the integrated intensities of the red and yellow bands of CL spectra obtained from the CdS window layer for different temperatures during the $CdCl_2$ treatment. The inset shows the same ratio as a function of the substrate temperature.

yellow CL bands are depicted as a function of the $CdCl_2$-processing temperature (T_{CdCl_2}) and of T_G for various samples. For values of T_{CdCl_2} smaller than 450 °C, the intensity ratio increases gradually and exhibits a steep increase for higher temperatures. A variation of T_G does not affect the intensity ratio of both CL bands as strongly as values of T_{CdCl_2} beyond 450 °C (cf. the inset of Fig. 9). The abrupt reduction of the conversion efficiency within the same range of T_{CdCl_2} suggests a correlation between passivation of the Cd interstitials of the CdS layer by $CdCl_2$ treatment and device performance. Further experiments are necessary to clarify to what extent the $CdCl_2$-related quenching of the yellow CL band in the CdS spectrum is actually linked to the abrupt decrease of the conversion efficiency of solar cells.

IV. CONCLUSIONS

The improvement of the conversion efficiency of CdS/CdTe solar cells related to $CdCl_2$ processing of the CdTe absorber layer correlates with homogenization of the spatial distribution of excitons bound to acceptors of CdTe. As a result, continuous *p*-type conversion of the polycrystalline CdTe is achieved. This result suggests chlorine is involved in the doping by the formation of a Cd vacancy–chlorine complex acting as an acceptor in CdTe. For substrate temperatures during the CdTe depositions (T_G) as high as 600 °C, a postdeposition $CdCl_2$ treatment does not significantly affect the intermixing at the CdS/CdTe interface even at treatment temperatures up to 460 °C. Instead, the electronic properties of the thin CdS window layer are strongly affected at those high treatment temperatures, suggesting a correlation with the strongly reduced conversion efficiency observed for the same conditions.

The width of the intermixed region in the vicinity of the CdS/CdTe interface of CdTe grains is clearly smaller than 100 nm for $T_G = 600$ °C and is on the order of a few 100 nm for $T_G = 630–650$ °C. Therefore, results of spatially integrating methods, which reveal widths of intermixed regions on the order of 1 μm or even wider, are strongly influenced by faster diffusion of sulfur in the grain boundaries and in other extended defects.

ACKNOWLEDGMENTS

The authors would like to thank H. T. Grahn for critical reading of the manuscript. This work was supported in part by the New Energy and Industrial Technology Development Organization (NEDO) as part of the New Sunshine Program under the Ministry of International Trade and Industry of Japan and also supported by a NEDO International Joint Research grant.

[1] J. Britt and C. Ferekides, Appl. Phys. Lett. **62**, 2851 (1993).
[2] De Vos, J. E. Parrot, P. Baruch, and P. T. Landsberg, *Proceedings of the 12th European Photovoltaic Solar Energy Conference, Amsterdam* (Stephens & Associates, Bedford, UK, 1994), p. 1315.
[3] K. Durose, P. R. Edwards, and D. P. Halliday, J. Cryst. Growth **197**, 733 (1999).
[4] P. R. Edwards, S. A. Galloway, and K. Durose, Thin Solid Films **361–362**, 364 (2000).
[5] A. L. Fahrenbruch, AIP Conf. Proc. **462**, 48 (1998).
[6] T. Okamoto, Y. Matsuzaki, N. Amin, A. Yamada, and M. Konagai, Jpn. J. Appl. Phys., Part 1 **37**, 3894 (1998).
[7] T. Okamoto, Y. Harada, A. Yamada, and M. Konagai, Sol. Energy Mater. Sol. Cells **67**, 187 (2001).
[8] K. A. Dhese, D. E. Ashenford, J. E. Nicholls, P. Devine, B. Lunn, C. G. Scott, and J. Jaroszynski, J. Cryst. Growth **138**, 443 (1994).
[9] J. S. Gold, T. H. Myers, N. C. Giles, K. A. Harris, L. M. Mohnkern, and R. W. Yanka, J. Appl. Phys. **74**, 6866 (1993).
[10] E. Molva, J. L. Pautrat, K. Saminadayar, G. Milchberg, and N. Magnea, Phys. Rev. B **30**, 3344 (1984).
[11] Among others, the detailed CL intensity fluctuation is influenced by the surface morphology. Thus, statements about concentration variations of acceptors are not possible.
[12] B. M. Basol, S. S. Ou, and O. M. Stafsudd, J. Appl. Phys. **58**, 3809 (1985).
[13] J. M. Figueroa, F. Sanchez-Sinencio, J. G. Mendoza-Alvarez, O. Zelaya, C. Vazquez-Lopez, and J. S. Helman, J. Appl. Phys. **60**, 452 (1986).
[14] S.-H. Wei and S. B. Zhang, *Proceedings of the 28th IEEE Photovoltaic Specialists Conference, Anchorage* (IEEE, New York, 2001).
[15] J. Schreiber, L. Hoering, H. Uniewski, S. Hildebrandt, and H. S. Leipner, Phys. Status Solidi A **171**, 89 (1999).
[16] K. Ohata, J. Saraie, and T. Tanaka, Jpn. J. Appl. Phys., Part 1 **12**, 1641 (1973).
[17] D. Grecu and A. D. Compaan, Appl. Phys. Lett. **75**, 361 (1999).
[18] D. W. Lane, G. J. Conibeer, D. A. Wood, K. D. Rogers, P. Capper, S. Romani, and S. Hearne, J. Cryst. Growth **197**, 743 (1999).
[19] R. Dhere *et al.*, *Proceedings of the 26th IEEE Photovoltaic Specialists Conference, Anaheim* (IEEE, New York, 1997), p. 435.
[20] M. Agata, H. Kurase, S. Hayashi, and K. Yamamoto, Solid State Commun. **76**, 1061 (1990).
[21] B. A. Kulp, Phys. Rev. **125**, 1865 (1962).
[22] K. D. Dobson, I. Visoly-Fisher, G. Hodes, and D. Cahen, Sol. Energy Mater. Sol. Cells **62**, 295 (2000).

Downloaded 18 Jun 2004 to 62.141.165.57. Redistribution subject to AIP license or copyright, see http://jap.aip.org/jap/copyright.jsp